LBL--21112

DE86 009908

Effects of Non-Condensible Gases on Fluid Recovery in Fractured Geothermal Reservoirs

Gudmundur S. Bodvarsson and Scott Gaulke, Earth Sciences Division, Lawrence Berkeley Laboratory, University of California, Berkeley, California 94720

Paper to be presented at the Society of Petroleum Engineers 56th Annual California Regional Meeting, April 2-4, 1986, Oakland, California.

ABSTRACT

Numerical simulations are performed in order to investigate the effects of noncondensible gases (CO_2) on fluid recovery and matrix depletion in fractured geothermal reservoirs. The model used is that of a well producing at a constant bottomhole pressure from a two-phase fractured reservoir. The results obtained have revealed a complex fracture-matrix interaction due to the thermodynamics of H_2O–CO_2 mixtures. Although the matrix initially contributes fluids (liquid and gas) to the fractures, later on, the flow directions reverse and the fractures backflow fluids into the matrix. The amount of backflow depends primarily upon the flowing gas saturation in the fractures; the lower the flowing gas saturation in the fractures the more backflow. It is shown that the recoverable fluid reserves depend strongly on the amount of CO_2 present in the reservoir system.

INTRODUCTION

Most geothermal fluids contain significant amounts of noncondensible gases. The concentration of gases in the steam at separator conditions are typically in the range of 2 - 8% by mass. Generally, carbon dioxide CO_2 constitutes over 90% of the gas; other gases include hydrogen sulfide H_2S. Gas concentrations often vary considerably across a geothermal field, hence, they can be useful tools in inferring flow patterns within the reservoir.[1] More importantly, however, the gases can affect the thermodynamic conditions within the reservoir that must be accounted for when gas-rich systems are being evaluated. Various studies have been published on the effects of noncondensible gases on well behavior and field wide response to exploitation.[2-9] Zyvoloski and O'Sullivan[3-5] and Grant[7] applied reservoir models including CO_2 to the Ohaaki reservoir in New Zealand. Atkinson et al.,[2] and Pruess et al.,[9] applied their models to two gas-rich Italian fields, the Bagnore reservoir and Larderello, respectively. Pritchett et al.,[6] and O'Sullivan, et al.,[8] performed generic studies of the effects of CO_2 on well testing results and the overall reservoir performance. All of these studies assumed porous medium behavior of the reservoir systems considered.

In the present paper we investigate the effects of CO_2 during exploitation of fractured geothermal reservoirs. Of particular interest are the matrix-fracture flow characteristics in such systems and the overall fluid recovery. Note that gas saturation is here defined as the pore volume fraction occupied by water vapor and CO_2 gas. The numerical studies were performed using the simulator MULKOM[10] with an equation of state for H_2O–CO_2 mixtures developed by O'Sullivan et al.[8] In this work we neglect effects of gaseous diffusion, capillary pressure and chemical reactions involving CO_2.

APPROACH

Most geothermal systems are located in volcanic rocks, where fractures provide fluids to the wells (Fig. 1). In most cases, geothermal wells have only a few major feed zones, so that the fracture spacing is on the order of tens or hundreds of meters. In the present work we employ a double porosity model based upon the MINC method.[11] We assume regular fracture geometry and spacing in a manner similar to the methodology developed by Warner and Root.[12] However, the MINC method allows for fully transient mass and heat flow between the fracture and the rock matrix.[11] The fractured porous medium grid is developed by a preprocessor program.[13]

The reservoir parameters considered in this study are given in Table 1. These parameters are typical for fractured geothermal reservoirs. The value used for the productivity index gives initial flow rates (30 - 40 kg/s), that are typical for high temperature geothermal wells. For the fracture relative permeabilities we assume linear curves with no residual liquid or gas (water vapor and CO_2); however, the conventional Corey curves are assumed for the porous rock matrix. In this

References and illustrations at end of paper.

DISCLAIMER

work gravity effects are neglected, so that the same initial conditions apply for both the fracture and matrix elements. An initial pressure of 90 bars, gas saturation of 20%, and a partial pressure of CO_2 of 10 bars are assumed. The initial temperature corresponding to these thermodynamic conditions is 295 °C. Note that many of the results given will be compared to a case with all the same parameters except that no gas is present (partial pressure of CO_2 equals zero). In this case the saturation temperature for an initial pressure of 90 bars is about 300 °C.

RESULTS

The simulations were carried out for a physical time exceeding 30 years. Figure 2 shows the flow rate transients at the well for the two cases (partial pressure of CO_2 of 0 and 10 bars). The figure shows a gradual decline in flow rate with time as expected for a well producing at a constant bottomhole pressure. The flow rate declines more rapidly for the case of no CO_2, because of more boiling, higher gas saturation and thus less overall fluid mobility. Figures 3 and 4 show the gas saturation transients for CO_2 partial pressures of 0 and 10 bars, respectively. The various curves represent fracture and matrix elements located at different radial distances from the well. Note that the matrix curves represent the matrix elements closest to the fractures; each matrix block is actually discretized into five different elements following the method of Pruess and Narasimhan.[11] From Figures 3 and 4 the following observations can be made. The fracture elements increase monotonically in gas saturation with time, but reach a quasi-steady state after a few years of production (after approximately 10^8 seconds). The stabilization time certainly depends on many of the problem parameters, but primarily upon the fracture spacing (or equivalently the surface area between fractures and rock matrix) and the matrix permeability. Basically the gas saturation in the fracture elements stabilizes when quasi-steady fluid and heat flow has been established between the fractures and the matrix. The gas saturation in the fracture elements stabilizes at considerably higher values when no CO_2 is present, or at about 70% compared to about 50% for a partial pressure of 10 bars.

The difference in the gas saturation transients for the two cases is much more pronounced for the rock matrix blocks. When no CO_2 is present the gas saturation in the matrix blocks increases drastically due to boiling, and high enthalpy fluids feed the fractures. On the other hand, when CO_2 is present, degassing occurs at early times, causing some of the pressure drop in the matrix, and then boiling increases the gas saturation to some extent. Still later, however, the gas saturation decreases again in the matrix, suggesting that a reversal in the fluid flow direction has occurred, so that fluids are now flowing from the fracture into the matrix. As shown in Figure 4, in the matrix elements shown actually contain more mass of fluid (lower gas saturation) at the end of the simulation than they initially contained. Figures 3 and 4 clearly show that the presence of CO_2 can have drastic effects upon the fluid recovery and matrix depletion.

The complex fracture-matrix interaction suggested by the results shown in Figures 3 and 4 can be explained in terms of the thermodynamics of H_2O–CO_2 systems, as described in the next section.

Figure 5 shows the enthalpy transients of the fluids feeding the well for the two cases. As expected, the fluid enthalpy for the no-CO_2 case is considerably higher than that for the case with a CO_2 partial pressure of 10 bars. This is because there is less boiling when CO_2 is present, and also because CO_2 has lower enthalpy than water vapor. Figure 5 also shows enthalpy enhancement at late times due to higher enthalpy fluids recharging the fracture system from the matrix, and also enthalpy enhancement due to conductive heat transfer from the matrix as the fluids flow in the fracture system towards the well.

Figure 6 shows the mass fraction of CO_2 in the produced fluids, both as a fraction of the total mass produced and as a fraction of the steam at the separators. In order to calculate the mass fraction of CO_2 in the steam at the separators, we assume isoenthalpic expansion of the fluids flowing up the wellbore, and a separator pressure 8 bars. Figure 6 shows that the mass fraction of CO_2 in the steam at the separators is about 6 - 7%, which compares well with data from gas-rich geothermal reservoirs. Note also that the CO_2 mass fraction starts to increase after a few months of production, because fluids recharging the fractures from the matrix contain more CO_2 than the fluids flowing within the fractures. Also note that at still later times the mass fraction of CO_2 starts to decline again, because of backflow into the rock matrix. This type of transient behavior of the gas concentration has been observed in several geothermal fields.[14]

FRACTURE-MATRIX FLOW IN H_2O–CO_2 SYSTEMS

In order to investigate the fracture-matrix flow in H_2O–CO_2 systems, let us consider a single matrix block surrounded by a fracture element (Fig. 7). For simplicity let us also assume that these elements are close to the well so that the thermodynamic conditions in the fracture element are constant and the pressure equals the bottomhole pressure. This approximation neglects early-time pressure and saturation transients in the fracture element, which are of no importance in the following discussion. The partial pressure of CO_2 and the gas saturation in the fracture element are also fixed at 2.8 bars and 50% respectively. These values correspond closely to the quasi-steady state conditions that developed in the fracture elements close to the well in the radial well problem described before.

The results of the transient changes in pressure, temperature, gas saturation and partial pressure of CO_2 in the matrix are shown schematically in Figure 8. Figure 9 shows schematically the changes in thermodynamic conditions of the matrix block on a pressure-temperature diagram. Note that the presence of CO_2 will lower the saturation temperature for a given pressure, and the more CO_2 is present, the lower the saturation temperature (Fig. 9). Based upon the two schematic figures the thermodynamic evolution of the matrix block can be understood.

Initially, a large pressure gradient exists between the fracture and the matrix so that fluids flow from the matrix to the fracture. This results in a declining pressure, boiling and a gradual rise in gas saturation. The partial pressure of CO_2 rapidly decreases because CO_2 flows with the gas phase out of the matrix. Boiling primarily generates water vapor since the

solubility of CO_2 in the liquid phase is small. After some time the pressure in the matrix block has declined to the fluid pressure in the fracture and there is almost no CO_2 in the matrix (the partial pressure of CO_2 is practically zero). At this time matrix conditions are at Point B in Figure 9, and the fracture and matrix are in pressure equilibrium but not in a temperature equilibrium, since there is gas in the fracture (the thermodynamic equilibrium state in the fracture corresponds to Point C in Fig.9). This causes conductive heat transfer between the fractures and the matrix. The conductive heat transfer gradually lowers the temperature in the matrix and consequently the pressure, because the matrix is under two-phase conditions. When the pressure in the matrix decreases below that in the fracture, mass flow of liquid and gas starts from the fracture into the matrix (backflow). This fluid contains CO_2 so that on the temperature-pressure diagram (Fig. 9), conditions are changing from Point B to Point C. The results from the simulations show that at all times during the backflow period the pressure in the matrix is a fraction of a bar below the fracture pressure. The backflow continues until enough CO_2 has flowed back into the matrix so that the partial pressure in the matrix is the same as the one in the fracture (Point C in Fig. 9). When this is achieved there is total thermodynamic equilibrium between the fracture and the matrix, i.e., equilibrium in pressure, temperature and partial pressure of CO_2.

DISCUSSION

Now that we have developed an understanding of the physics controlling the flow characteristics in H_2O–CO_2 systems, it is important to relate it to the more realistic radial well problem discussed before. Figures 10 and 11 show schematically fluid flow patterns in the geothermal reservoirs for the two cases of no CO_2 and 10 bar CO_2 partial pressure, respectively. Figure 10 shows the conventional flow characteristics in fractured porous media produced at a constant downhole pressure. Near the well, the fractures and the rock matrix have reached equilibrium pressure conditions, and the only interchange between fluids flowing to the well and the rock matrix is enthalpy enhancement due to conductive heat transfer. Away from the well the rock matrix is providing fluids and heat to the fractures, similar to production of any one-component fluid (e.g., oil, gas, etc.). The region where fluid recharge from the matrix is taking place is gradually moving away from the well. Figure 11 illustrates a different phenomenon that is caused by the multi-component (H_2O–CO_2) environment. Away from the well the matrix recharges fluids to the fractures, in a manner similar to that described for the no-CO_2 case. Closer to the well, however, there is non-equilibrium in temperature, and concentration of CO_2, that causes backflow of fluids into the rock matrix. Very near the well one may expect that total equilibrium has been achieved, with pressures, temperatures and CO_2 partial pressures equal in the fractures and the rock matrix.

Figure 12 shows the variations in the average matrix gas saturation with radial distance from the well for our radial well problem (described before). Gas saturation profiles are given for different times ranging from 1 to 30 years. The figure shows clearly that considerable backflow is occurring, especially after five years of production.

The amount of backflow into the matrix depends on various factors, the most important of which is probably the flowing gas saturation in the fractures. The lower the flowing gas saturation in the fractures the more backflow is required to achieve equilibrium of the partial pressure of CO_2 , since most of the CO_2 is in the gas phase. Figure 13 shows an example of where the backflow into the matrix is so strong that the matrix block contains more fluid mass in its final equilibrium state than it did initially. In this case we assumed a rather low stable flowing gas saturation in the fracture. Early in the evolution the matrix block loses about 50% of the initial mass in place, but then the strong backflow causes it to end up with 10% more fluid mass than it had originally.

The flowing CO_2 mass fraction in the fractures does not greatly affect the amount of backflow, if the mass fraction remains fairly constant. High CO_2 mass fraction in the fracture fluids requires less fluid flow into the fractures to equilibrate the CO_2 partial pressures. On the other hand, if the CO_2 mass fraction is low, then only a small amount of CO_2 is needed. Changes in the flowing CO_2 mass fraction can have significant effects in the stable gas saturation in the matrix.

If the mass fraction of CO_2 in the fracture declines with time, perhaps due to a localized two-phase or upflow zone, additional fluid recovery from the matrix will be realized. On the other hand, an increasing CO_2 concentration in the produced fluids, perhaps due to the presence of a two-phase zone near a fresh intrusion (magma), will require an increasing partial pressure of CO_2 in the matrix, by backflow from the fractures into the matrix.

Thus, injection of fluids with low gas concentration may significantly improve fluid recovery from matrix blocks. Injection will reduce the CO_2 concentration in the fracture system, thus enhancing additional fluid flow from the matrix.

Figure 14 shows the effects of initial CO_2 partial pressure on the gas saturation transients in the matrix. The figure demonstrates clearly the effects of CO_2 on the fluid recovery from the matrix. In this case the backflow is not very significant because of the rather high flowing gas saturation in the fractures.

It should be noted that in the present work we have not considered gaseous diffusion, capillary pressure effects or reactions involving CO_2. Gaseous diffusion tends to equilibrate chemical gradients and should therefore not affect the general conclusions of this work but only the time frame. Capillary pressure gradients caused by gradients in gas saturation are certainly important at low temperatures, but may not be very important at high temperatures.[15] Reactions involving CO_2 may be very important in some geological environments where carbonates are abundant.[9]

CONCLUSIONS

Numerical simulation techniques are employed in order to investigate the effects of CO_2 on fluid recovery and reservoir depletion in fractured two-phase geothermal reservoirs. The main results obtained are as follows:

(1) CO_2 greatly affects the fluid recovery from matrix blocks. The higher the initial partial pressure of CO_2 the less the recoverable reserves.

(2) CO_2 causes backflow from the fractures into the rock matrix at late times that reduces the recovery of the fluid reserves. The backflow is caused by the complex thermodynamics of H_2O–CO_2 systems.

(3) The amount of backflow depends primarily upon the flowing gas saturation and the mass fraction of CO_2 in the fractures. The backflow is not very important for high enthalpy (steam) wells, but can be substantial for low enthalpy wells.

(4) Reinjection of fluids of low gas concentration will help increase the recoverable reserves and energy of the system.

ACKNOWLEDGEMENTS

The authors acknowledge technical review of this manuscript by M. J. Lippmann. They also thank K. Pruess for allowing use of the software MULKOM and the MINC preprocessor program. This work was supported through U.S. Department of Energy Contract No. DE-AC03-76SF00098 by the Assistant Secretary for Conservation and Renewable Energy, Office of Renewable Technology, Division of Geothermal Technology.

REFERENCES

1. Armannsson, H., Gislason, G., and Hauksson, T.: "Magmatic Gases in Well Fluids Aid the Mapping of the Flow Pattern in a Geothermal System," *Geochimica et Cosmochimica Acta,* (1982) **46,** 167-177.

2. Atkinson, P. G., Celati, R., Corsi, R., and Kucuk, F.: "Behavior of the Bagnore Steam/CO_2 Geothermal Reservoir, Italy," *Soc. Pet. Eng. J.,* (1980) **20** No. 4, 228-238.

3. Zyvoloski, G. A., and O'Sullivan, M. J.: "Simulation of a Gas-Dominated, Two-Phase Geothermal Reservoir," *Soc. Pet. Eng. J.,* (1980) **20** No. 1, 52-58.

4. Zyvoloski, G. A., and O'Sullivan, M. J.: "A Simple Model of the Broadlands Geothermal Field," *N. Z. J. Sci.,* (1978) **21,** 505-510.

5. Zyvoloski, G. A., and O'Sullivan, M. J.: "Simulation of the Broadlands Geothermal Field, New Zealand," Proceedings 4th Workshop Geothermal Reservoir Engineering, Stanford, (1978) 332-342.

6. Pritchett, J. W., Rice, M. H., and Riney, T. D.: "Equation-of-State for Water-Carbon Dioxide Mixtures: Implications for Baca Reservoir," Report prepared by Systems, Science and Software, La Jolla, California (1981).

7. Grant, M. A.: "Broadlands - A Gas Dominated Geothermal Field," *Geothermics,* (1977) **6,** No. 1, 9-29.

8. O'Sullivan, M. J., Bodvarsson, G. S., Pruess, K., and Blakeley, M. R.: "Fluid and Heat Flow in Gas-Rich Geothermal Reservoirs," *Soc. Pet. Eng. J.,* (1985) **25,** No. 2, 215-226, LBL-16329.

9. Pruess, K., Celati, R., Calore, C., and D'Amore, F.: "CO_2 Trends in the Depletion of the Larderello Vapor-Dominated Reservoir, Proc. Tenth Workshop Geothermal Reservoir Engineering, Stanford, CA, report SGP-TR-84, (1985), 273-278, LBL-19092.

10. Pruess, K.: "Development of the General Purpose Simulator MULKOM," 1982 Annual Report, Earth Sciences Division, Lawrence Berkeley Laboratory, Berkeley, CA.

11. Pruess, K., and Narasimhan, T. N: "On the Fluid Reserves and the Production of Superheated Steam From Fractured Vapor-Dominated Geothermal Reservoirs, *J. Geo. Res.,* (1982) **87,** No. B11, 9329-9339.

12. Warren, J. E., and Root, P. J.: "The Behavior of Naturally Fractured Resevoirs," *Soc. Pet. Eng. J.,* (1963) 245-255.

13. Pruess, K.: "GMINC - A Mesh Generator for Flow Simulations in Fractured Reservoirs," Lawrence Berkeley Laboratory Report, LBL-15227, Berkeley, CA, (1983) 64 pp.

14. D'Amore, F., and Truesdell, A. H.: "Models for Steam Chemistry at Larderello and The Geysers," Proc. Fifth Workshop Geothermal Reservoir Engineering, Stanford, CA, (1979) 283-297.

15. Cady, G. V.: "Model Studies of Geothermal Fluid Production," Ph.D. Thesis, Stanford University, Stanford, California (1969).

Table 1. Parameter values used in the study.

Parameter	Value
Reservoir thickness	1000 m
Wellbore radius	0.1 m
Bottomhole pressure	40 bars
Productivity Index	1.25×10^{-12} m^3
Fracture spacing	100 m
Fracture porosity	1%
Matrix porosity	5%
Fracture transmissivity	2.0 Darcy meters
Matrix permeability	.01 md
Thermal conductivity	2.0 W/m·°C
Rock heat capacity	1000 J/kg·°C
Rock density	2650 kg/m^3
Fracture relative permeability	X-curves with S_{lr}=.0, S_{gr}=.0
Matrix relative permeability	Corey-curves with S_{lr}=.75, S_{gr}=.25
Initial pressure	90 bars
Initial gas saturation	20%
Initial partial pressure of CO_2	10 bars (or 0 bars)
Initial temperature	295 °C (or≈300 °C)

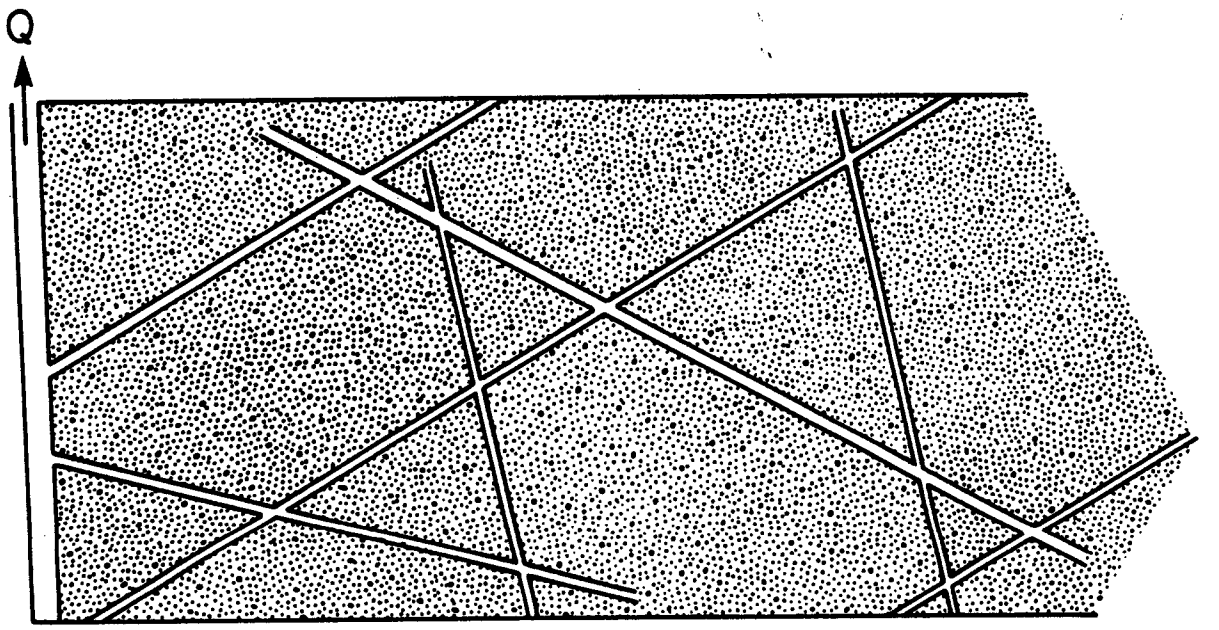

XBL 861-10550

Figure 1. A model of a fractured porous geothermal reservoir.

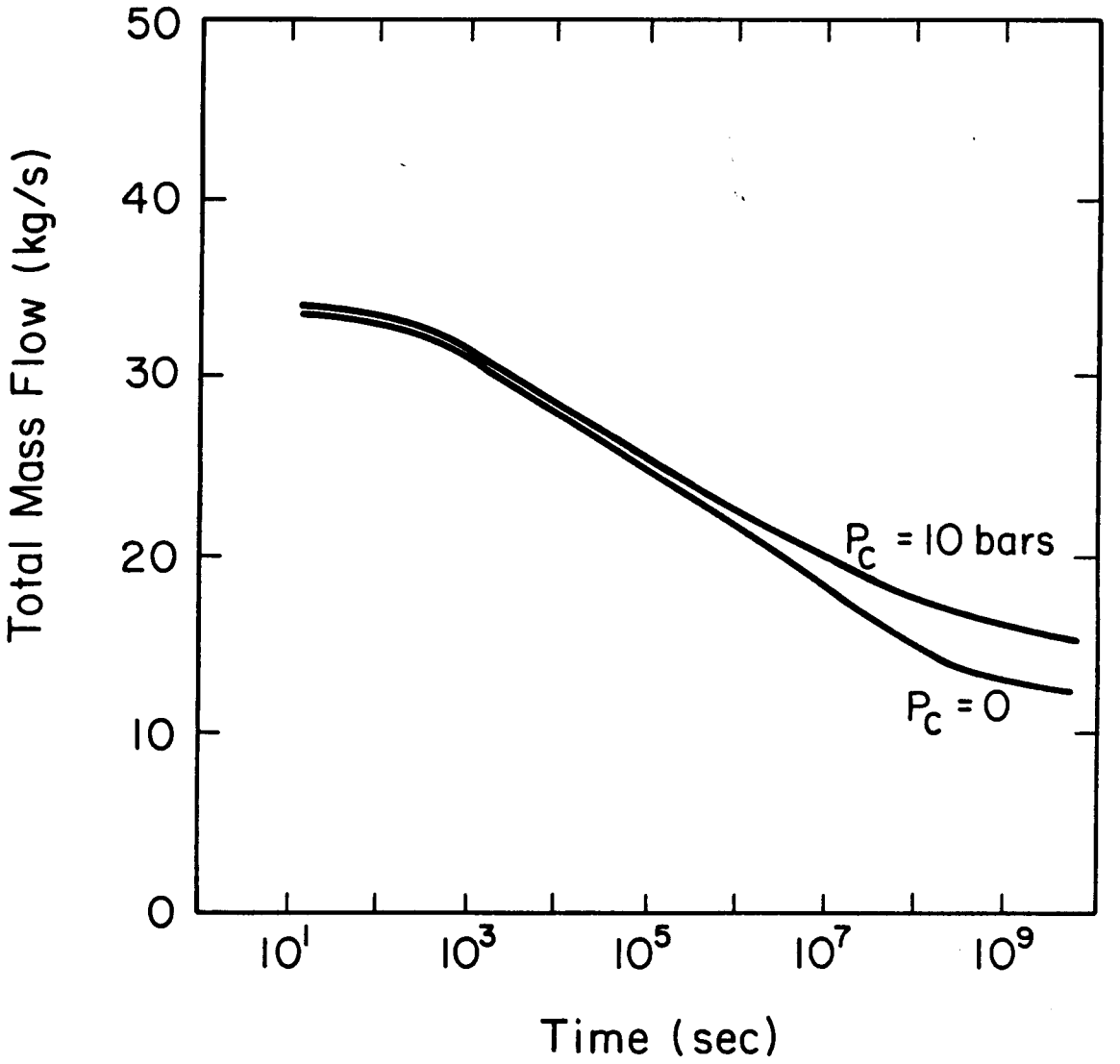

Figure 2. Changes in flow rate with time for the cases of no CO_2 and 10 bar CO_2 partial pressure.

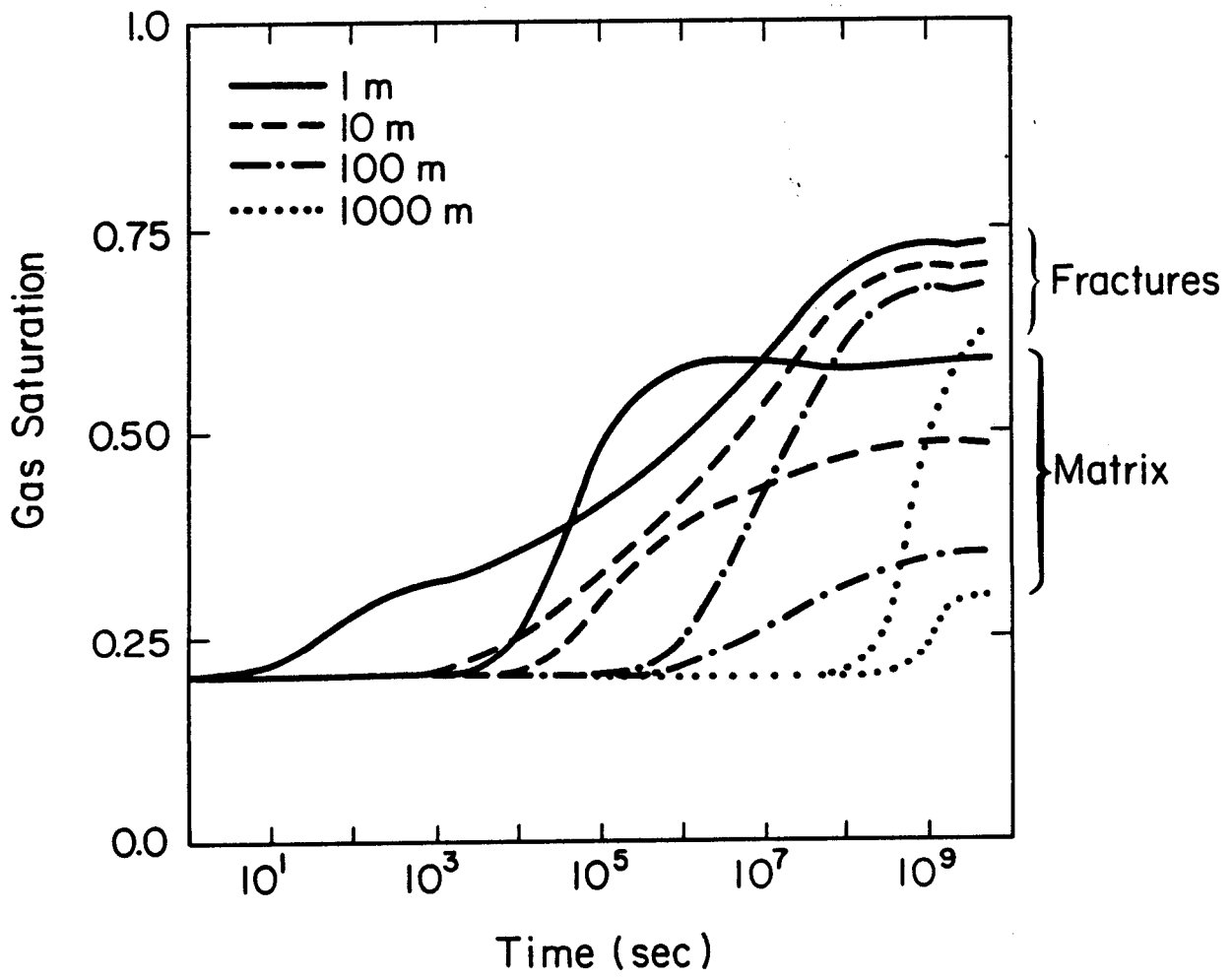

Figure 3. Changes in gas saturation with time for various fracture and matrix elements (no CO_2).

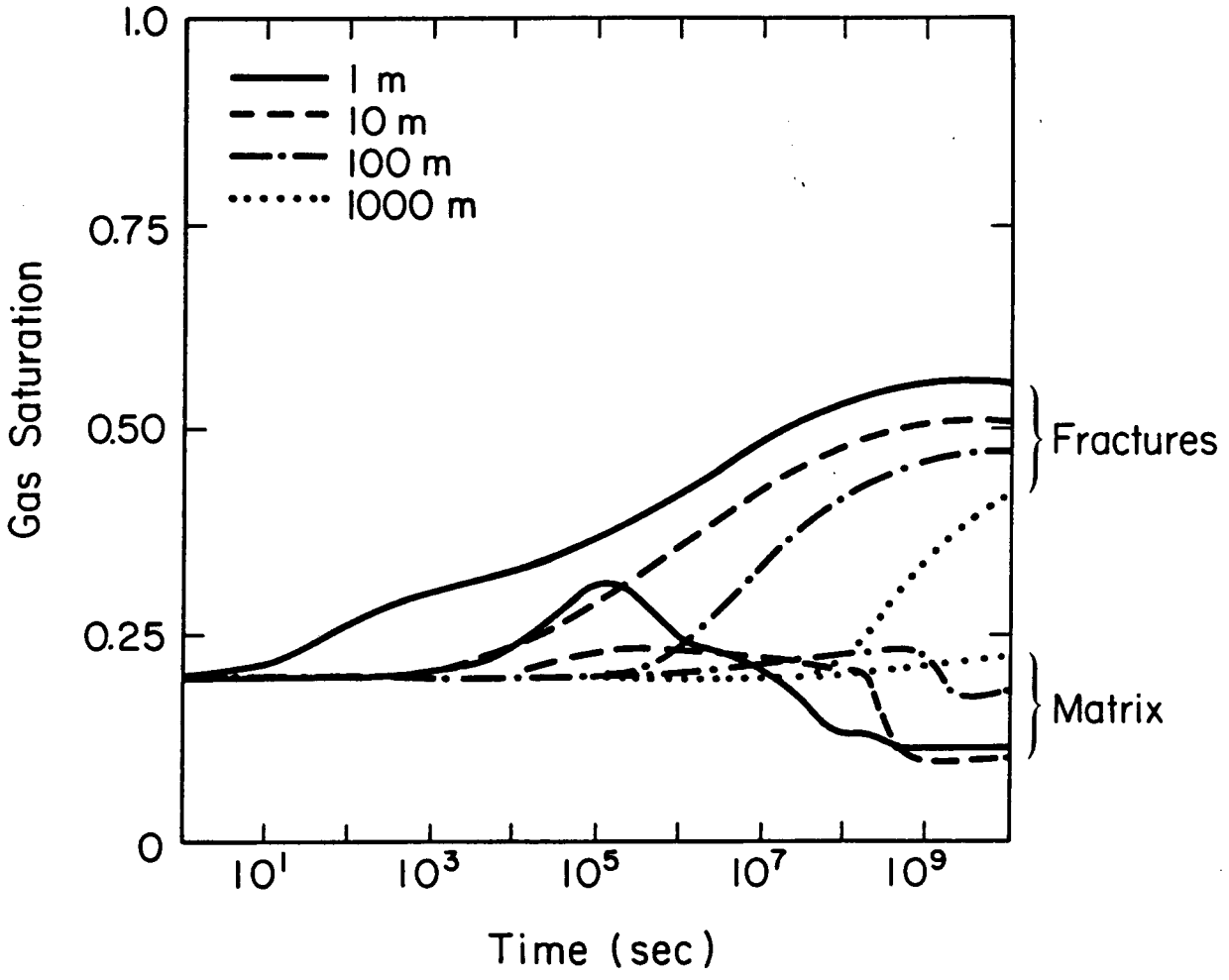

Figure 4. Changes in gas saturation with time for various fracture and matrix elements (CO_2 partial pressure of 10 bars).

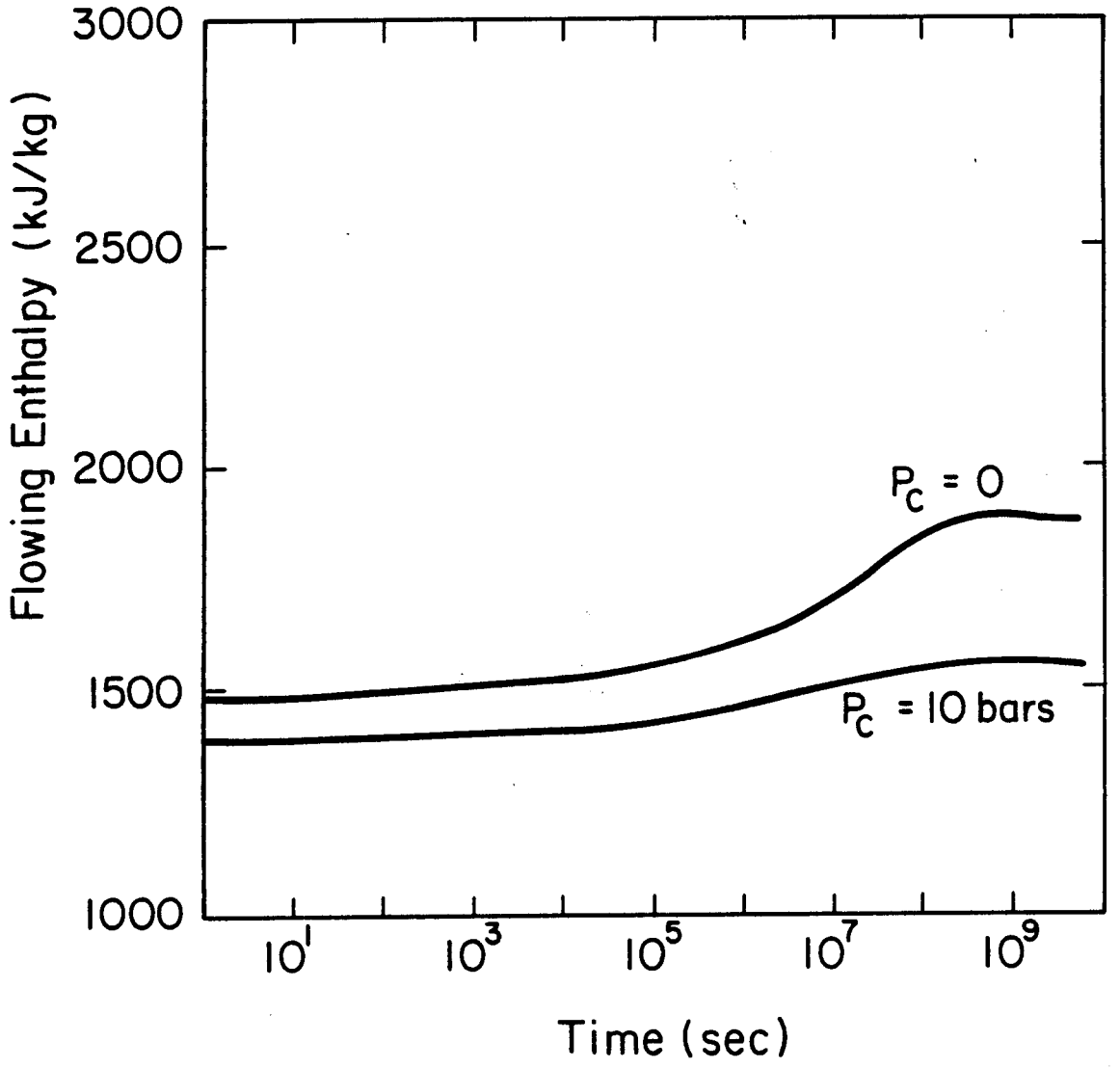

Figure 5. Changes in flowing enthalpy with time for the cases of 0 and 10 bar CO_2 partial pressure.

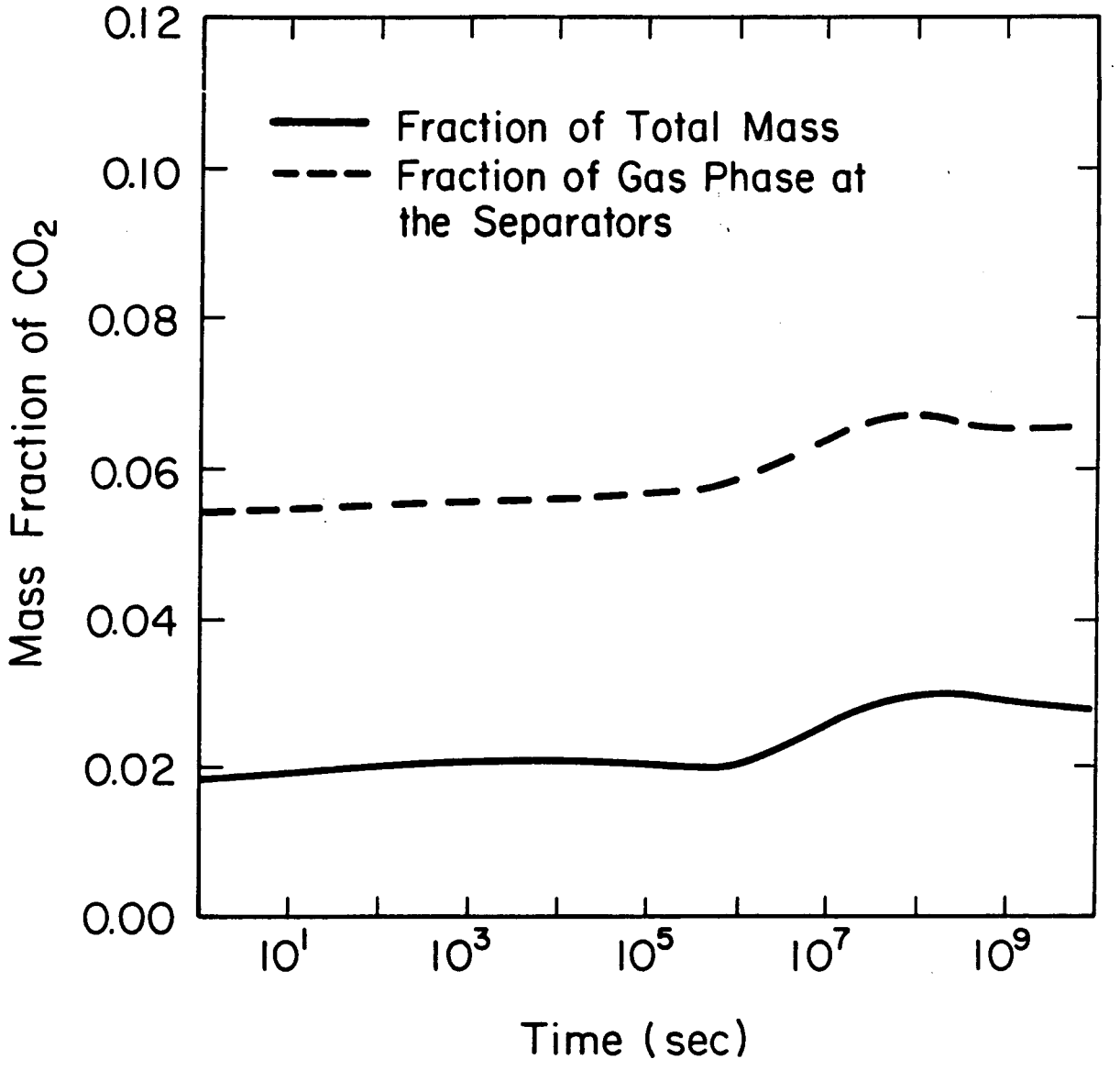

Figure 6. Changes in CO_2 mass fraction with time.

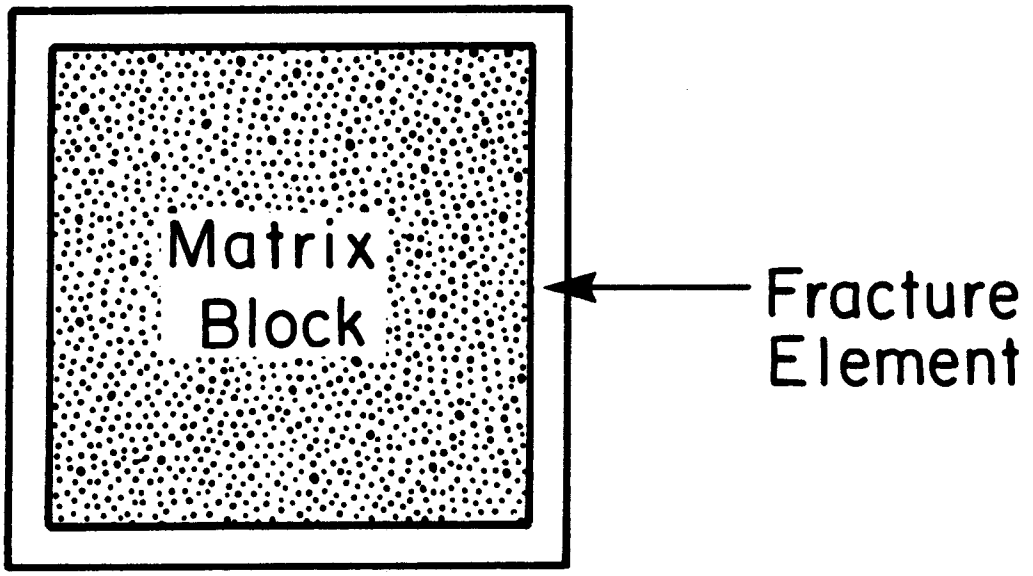

XBL 861-10559

Figure 7. Simple model of a matrix block surrounded by a fracture.

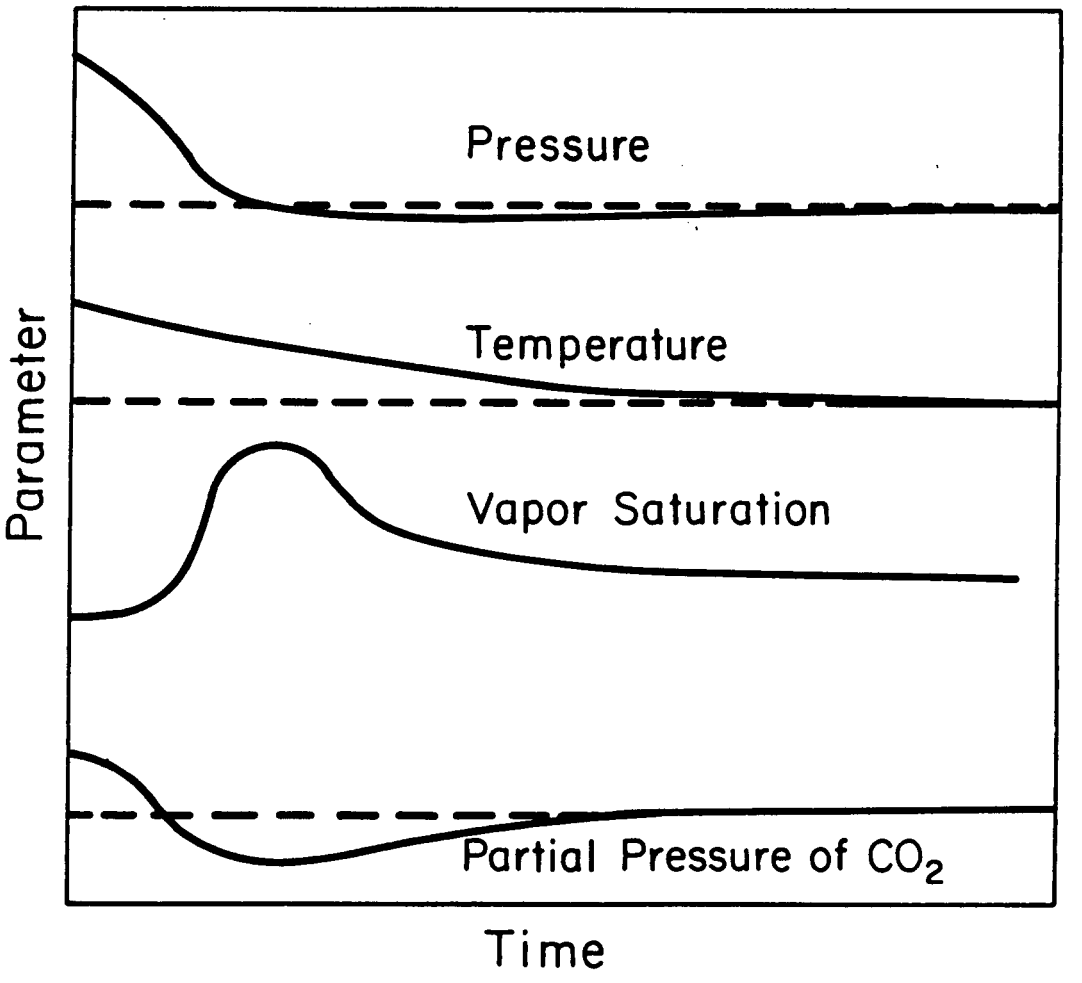

Figure 8. Schematic results of changes in pressure, gas saturation, temperature and CO_2 partial pressure with time in the matrix.

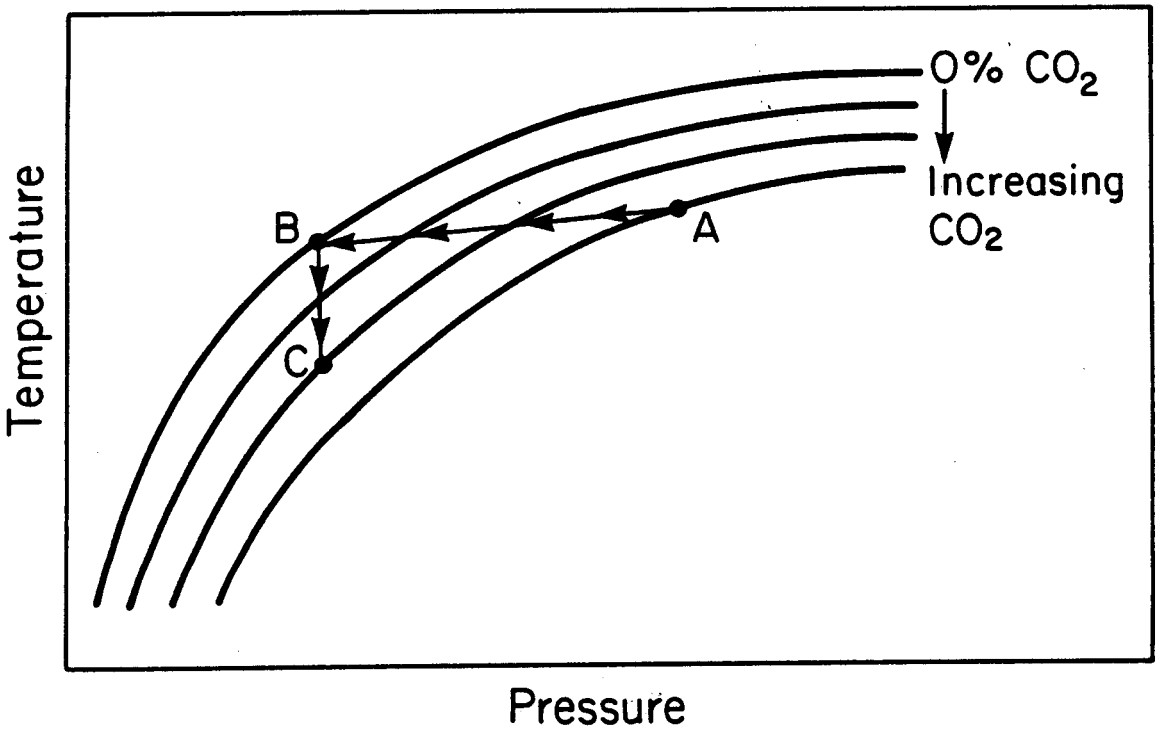

Figure 9. Schematic diagram of pressure-temperature relationship for H_2O–CO_2 systems.

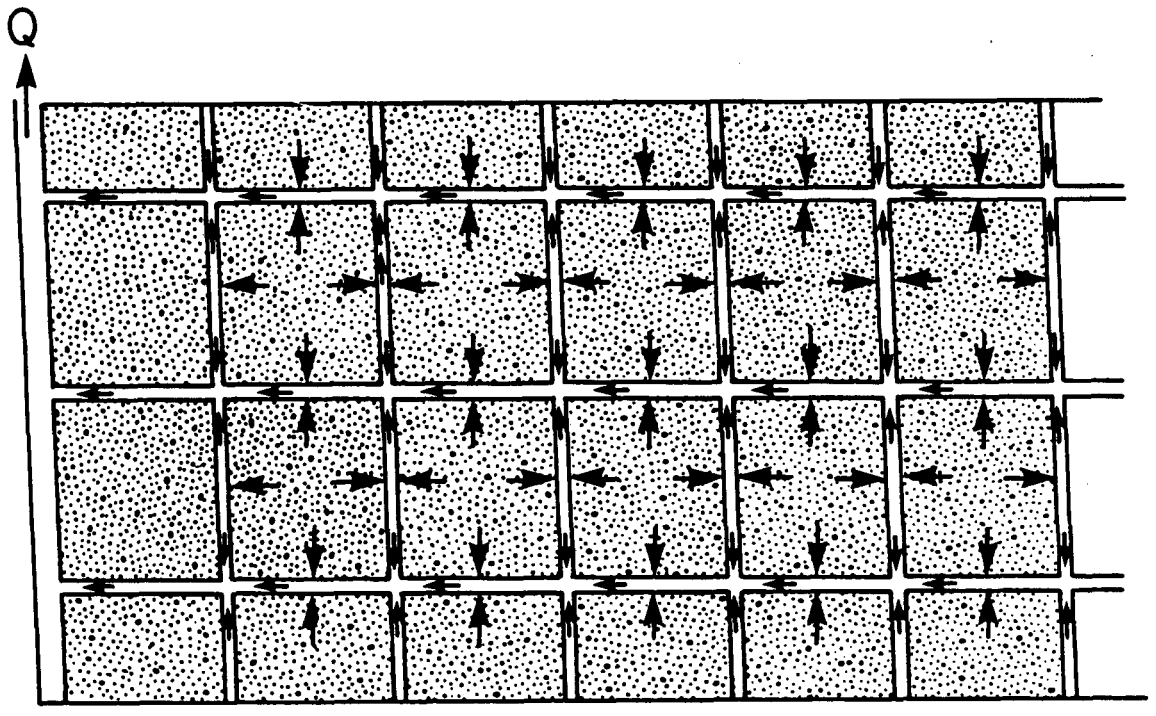

XBL 861-10551

Figure 10. Schematic view of fracture-matrix flow in a geothermal reservoir with no CO_2.

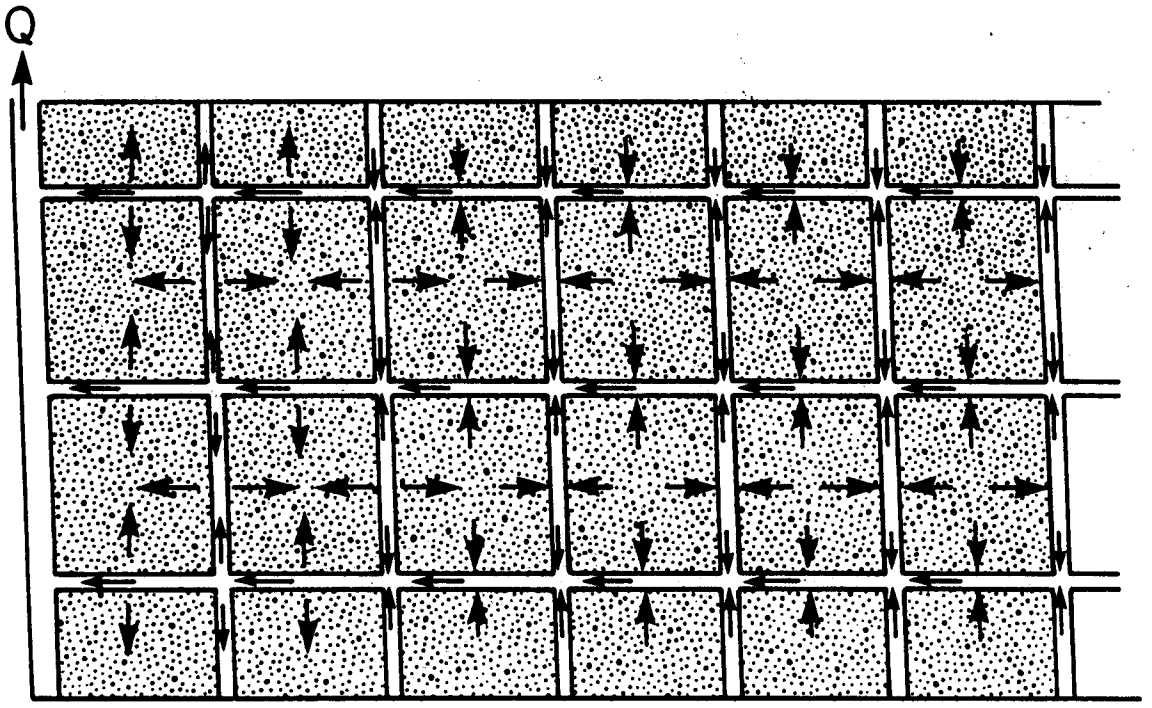

XBL 861-10552

Figure 11. Schematic view of fracture-matrix flow in a gas-rich reservoir.

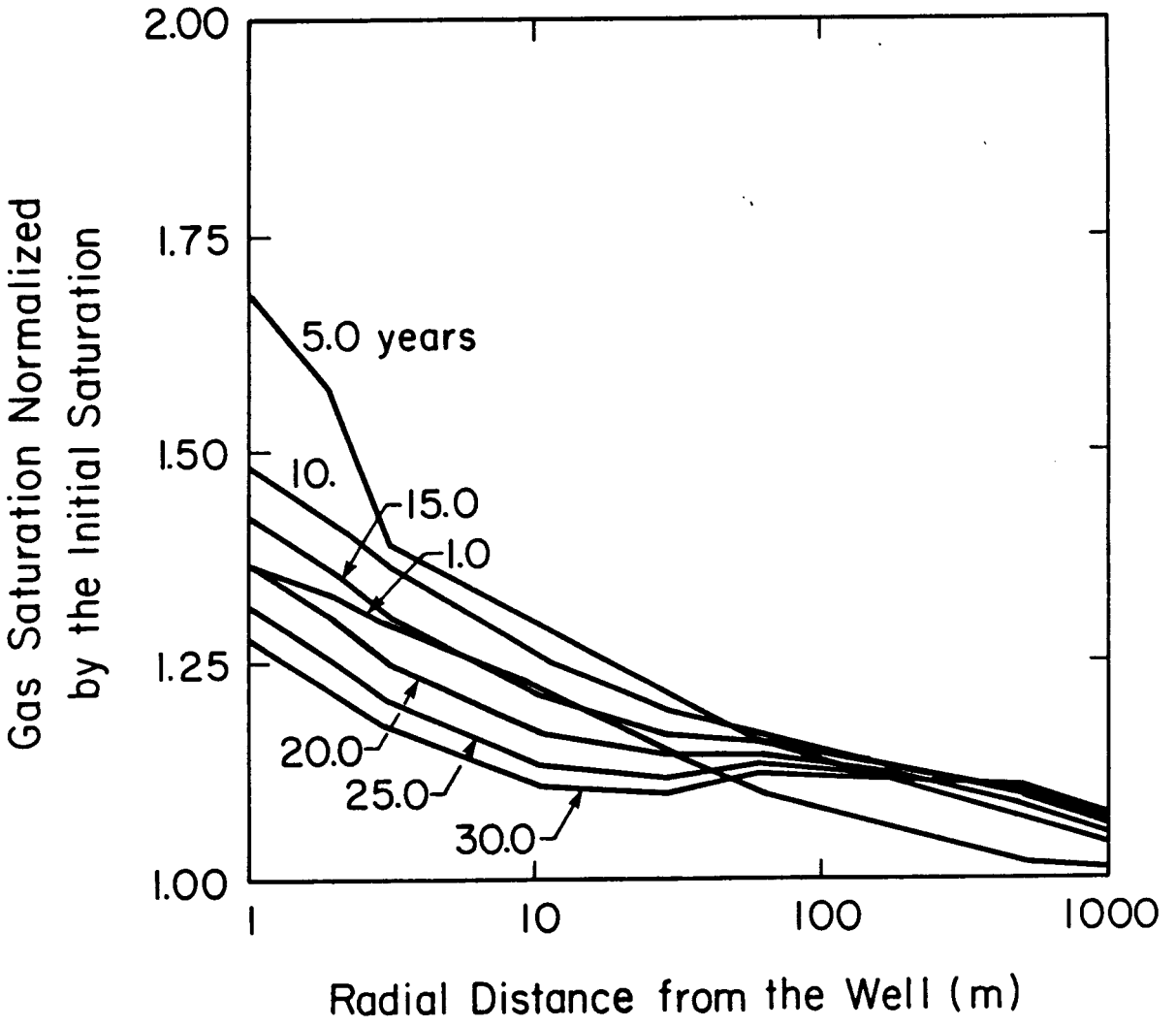

Figure 12. Variations in the average matrix gas saturation with radial distance from the well.

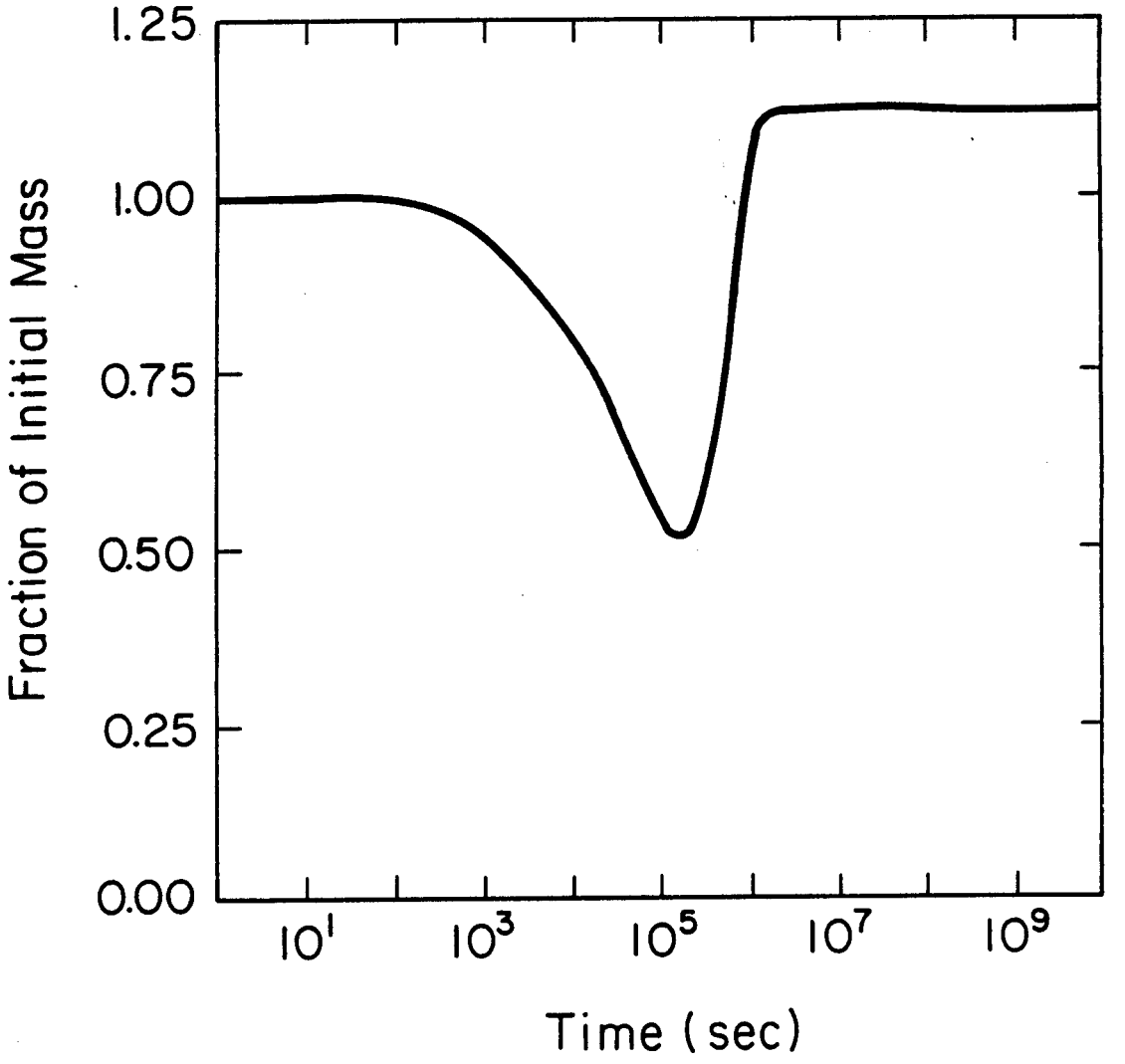

Figure 13. Results of a two element problem with large backflow into the matrix.

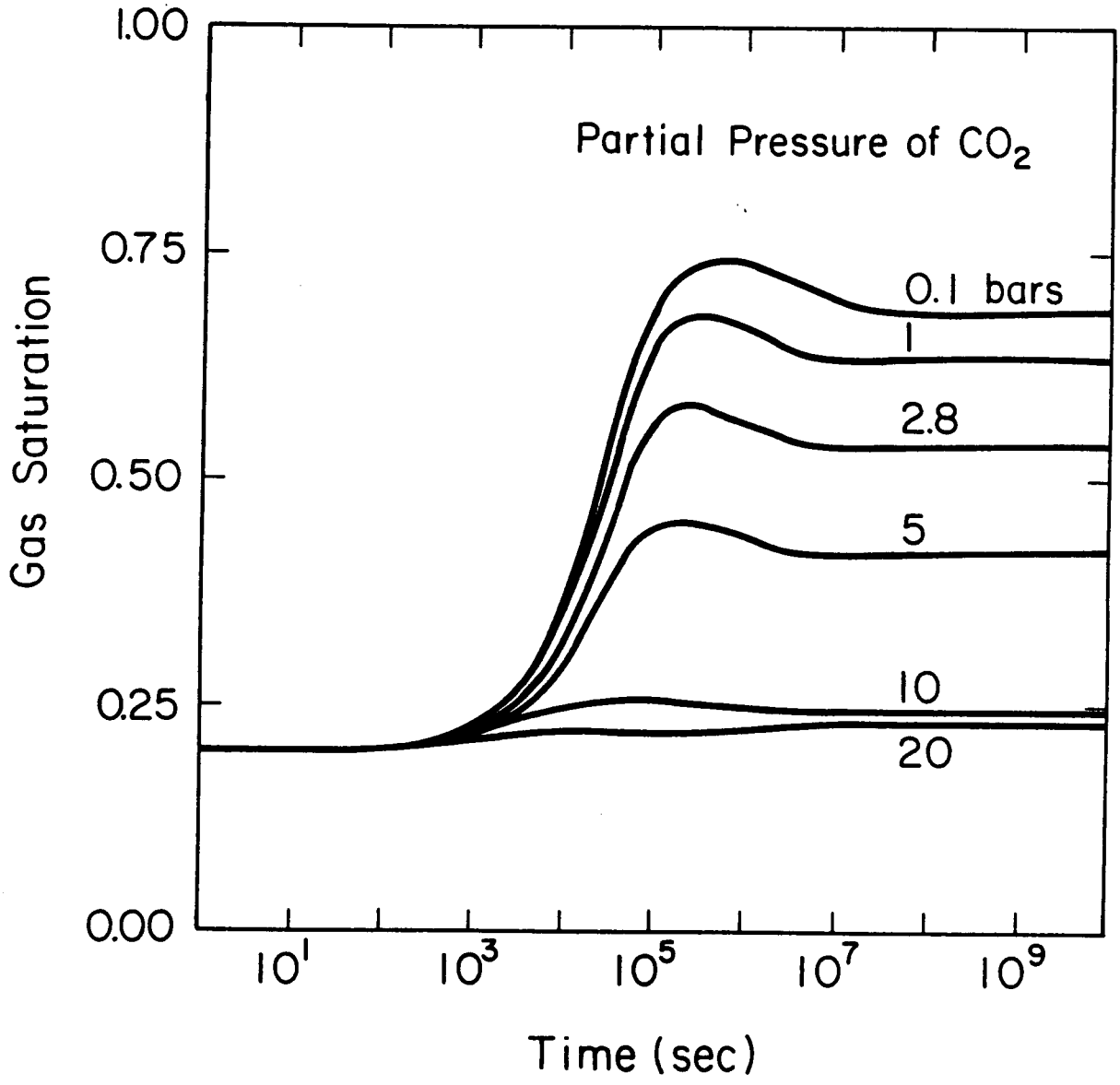

Figure 14. Effects of CO_2 partial pressure on the gas saturation transients in the matrix.